Available online at www.sciencedirect.com

ScienceDirect

Remote Sensing of Environment 112 (2008) 1010–1024

Remote Sensing of Environment

www.elsevier.com/locate/rse

Mapping plant functional types from MODIS data using multisource evidential reasoning

Wanxiao Sun [a,*], Shunlin Liang [b], Gang Xu [a], Hongliang Fang [b], Robert Dickinson [c]

[a] Department of Geography and Planning, Grand Valley State University, MI, USA
[b] Department of Geography, University of Maryland, MD, USA
[c] School of Earth and Atmospheric Sciences, Georgia Institute of Technology, GA, USA

Received 5 October 2006; received in revised form 31 March 2007; accepted 15 July 2007

Abstract

Reliable information about the geographic distribution and abundance of major plant functional types (PFTs) around the world is increasingly needed for global change research. Using remote sensing techniques to map PFTs is a relatively recent field of research. This paper presents a method to map PFTs from the Moderate Resolution Imaging Spectroradiometer (MODIS) data using a multisource evidential reasoning (ER) algorithm. The method first utilizes a suite of improved and standard MODIS products to generate evidence measures for each PFT class. The multiple lines of evidence computed from input data are then combined using Dempster's Rule of combination. Finally, a decision rule based on maximum support is used to make classification decisions. The proposed method was tested over the states of Illinois, Indiana, Iowa, and North Dakota, USA where crops dominate. The Cropland Data Layer (CDL) data provided by the United States Department of Agriculture were employed to validate our new PFT maps and the current MODIS PFT product. Our preliminary results suggest that multisource data fusion is a promising approach to improve the mapping of PFTs. For several major PFT classes such as crop, trees, and grass and shrub, the PFT maps generated with the ER method provide greater spatial details compared to the MODIS PFT. The overall accuracies increased for all the four states, with the biggest improvement occurring in Iowa from 51% (MODIS) to 64% (ER). The overall kappa statistic also increased for all the four states, with the biggest improvement occurring in Iowa from 0.03 (MODIS) to 0.38 (ER). The paper concludes with a discussion of several methodological issues pertaining to the further improvement of the ER approach.

Keywords: Plant functional type (PFT); Data fusion; Evidential reasoning; Dempster–Shafer theory of evidence; Evidence measures; MODIS data

1. Introduction

Plant functional types (PFT) are groups of plant species that share similar functioning at the organismic level, similar responses to environmental factors, and/or similar effects on ecosystems (Smith et al., 1997). Reliable information about the geographic distribution and abundance of major PFTs around the globe is increasingly needed for global change research. For example, the National Center for Atmospheric Research land surface model (NCAR LSM) has shifted from using biome-based land cover information to using satellite-derived PFT maps (Bonan et al., 2002; Tian et al., 2004). The carbon models used to scale carbon fluxes also typically require specification of PFTs (Denning et al., 1996; Sellers et al., 1997). Using remote sensing techniques to extract reliable PFT information can therefore contribute to improved predictive capabilities of global and regional carbon cycle, climate and ecosystem models.

The increased utilization of PFT information stems from the realization that traditional biome-based land cover characterization can no longer meet the needs of recent advances in global change research. For example, most land models are expanding beyond their traditional biogeophysical roots to include biogeochemistry, especially photosynthesis and the carbon cycle (Bonan, 1996; Dickinson et al., 1998; Foley et al., 1996; Kucharik et al., 2000). Inclusion of photosynthesis and the carbon cycle in land models requires specification of many leaf-level and whole-plant physiological parameters. The

* Corresponding author.
E-mail address: sunwa@gvsu.edu (W. Sun).

0034-4257/$ - see front matter © 2007 Elsevier Inc. All rights reserved.
doi:10.1016/j.rse.2007.07.022

functions are very difficult to be parameterized in the case of mixed life-form biomes such as savannas and mixed forests, because a mixed life-form biome consists of physiologically distinct plant species.

Representing vegetation as patches of PFTs offers several important advantages over the biome-based land classification approach (Bonan et al., 2002). First, PFT provides a direct link to leaf-level physiological measurements, making it possible to more accurately set vegetation parameters in land models. Second, PFT allows modelers to more accurately represent the land surface by separately specifying the composition and structure of PFTs within a grid cell. Third, representing vegetation in terms of PFTs also allows land models to better interface with ecosystem dynamics models, because the latter typically simulate vegetation change in terms of the abundance of PFTs (Gamon et al., 2004; Running & Coughlan, 1988; Sitch et al., 2003; Smith et al., 2001).

The Moderate Resolution Imaging Spectroradiometer (MODIS) Land Team is producing a global PFT map (i.e., MODIS Land Cover Type 5) for use in the Community Land Model (CLM) (http://edcdaac.usgs.gov/modis/mod12q1v4.asp). This PFT product is generated by re-labeling the International Geosphere–Biosphere Programme (IGBP) classes of MODIS Land Cover Type 1 product (Friedl et al., 2002; Strahler et al., 1999). The MODIS PFT is the only global PFT data set currently available. However, the error magnitudes of the MODIS PFT product and their spatial and temporal distributions have not been fully characterized. Errors and uncertainties in PFT data can multiply and compromise the credibility of global change research. Several studies have demonstrated that the use of different PFT data sets has a significant effect on climate modeling results (e.g., Bonan et al., 2002; Oleson & Bonan, 2000; Tian et al., 2004).

The increased availability and information content of remotely sensed data being generated by Earth Observing System (EOS) sensors and other sensors has provided considerable potential for the extraction of PFT information. However, due to the enormous diversity of terrestrial plant species and the spatial and temporal variability in the morphological and spectral characteristics of PFTs, accurate mapping of PFTs over large areas is a difficult task (Box, 1996; Prentice et al., 1992; Semenova & van der Maarel, 2000; Smith et al., 1997). Sun and Liang (2007) recently discussed several methodological issues pertaining to the mapping of PFTs over large areas. Their study shows that at the present time no satisfactory methodology exists for the extraction of PFTs from satellite observations. A main conclusion from their study is that incorporation of a wide array of information including both satellite observations and ancillary data into PFT classification procedures is indispensable to improved mapping of PFTs at continental to global scales.

In this paper we report some preliminary results from an ongoing research that aims to map PFTs from MODIS data using a data fusion approach. The main idea behind our methodology is that since a PFT has its manifestations in multiple domains such as plant physiognomy, vegetation structure, phenology, and environmental conditions (Running et al., 1995), the use of multiple lines of evidence reflecting the characteristics of a PFT in the above domains should help enhance the ability to extract PFTs. In this research, the evidence used to discern PFTs is generated from a suite of improved and standard MODIS products including LAI, EVI and albedos. The multiple lines of evidence computed from the input data are then fused using an evidential reasoning algorithm.

Evidential reasoning is a method of inexact reasoning (Giarratano & Riley, 1998; Peddle, 1995a,b). The method is based on the recognition that the knowledge and information we use in making decisions such as image classification is often uncertain, incomplete, and occasionally imprecise. As such, the method is designed to capture the natural behavior of reasoning by narrowing the hypothesis set down to a smaller number of possibilities as evidence increases (Lein, 2003). Evidential reasoning has been used in a variety of earth resources and geoscience applications, such as geological mapping (Moon, 1990, 1993), water resources (Caselton & Luo, 1992; Peddle & Franklin, 1993), forestry mapping (Goldberg et al., 1985), sea ice identification (Soh et al., 2004), and land cover classification (Cohen & Shoshany, 2005; Lee et al., 1987; Lein, 2003; Peddle, 1995a,b; Srinivasan & Richards, 1990). Past research has shown that evidential reasoning can produce more accurate results compared to traditional classifiers (Le Hégarat-Mascle et al., 2003; Lein, 2003; Peddle, 1995a,b; Soh et al., 2004).

The proposed method is tested over the states of Illinois, Indiana, Iowa, and North Dakota, USA. These four states represent an important type of landscape of the United States where crops dominate. The Cropland Data Layer (CDL) data provided by the National Agricultural Statistic Service of the U.S. Department of Agriculture are used to validate our results.

2. PFT classification scheme, input data, and reference data

The PFT classification scheme used in this study is the same as the one used in the MODIS PFT product. The MODIS PFT scheme consists of 12 classes including water, evergreen needleleaf trees, evergreen broadleaf trees, deciduous needleleaf trees, deciduous broadleaf trees, shrub, grass, cereal crop, broadleaf crop, urban and built-up, snow and ice, and barren or sparse vegetation.

Nine MODIS data sets are used in this study as the sources of evidence. These include improved MODIS LAI, MODIS EVI (MOD13A2), and seven spectral bands of MODIS “black-sky” albedo (MOD43B3) for the year 2001. The choice of these input data sets is based primarily on their utility for the recognition and discrimination of different PFTs. MODIS Leaf Area Index (LAI) and MODIS Enhanced Vegetation Index (EVI) are chosen because they contain information about the properties of different PFTs in terms of their plant physiognomy (e.g., canopy structure and leaf longevity), vegetation structure (e.g., fractional vegetation cover), and phenology (e.g., onset and duration of greenness). MODIS albedo products can also aid the discrimination of PFTs because they contain spectral information about land surface properties under perfect scattering conditions. A more detailed discussion of the utility of MODIS products as sources of evidence for mapping PFTs can be found in Sun and Liang (2007).

The quality of MODIS products is also taken into account in choosing of input data. For example, we use the improved MODIS LAI product, instead of the standard MODIS LAI product (MOD15A2), because the latter product is full of gaps and low quality pixels. The improved MODIS LAI product is more accurate and continuous in both time and space (Fang et al., in press). Forty six improved 8-day MODIS LAI images, 23 16-day MODIS EVI images and 23 16-day images of each of the seven MODIS albedo products are employed as evidence layers in this study. The standard MODIS PFT product is also used in combination with the above MODIS products to generate evidence measures for each PFT class.

The Cropland Data Layer (CDL) data for 2001 were used as reference data in this study. Note that both the MODIS input data sets (i.e., evidence layers) and the reference data were captured in the same year. The CDL data was provided by the National Agricultural Statistics Services (NASS) of the U.S. Department of Agriculture (USDA) (http://www.nass.usda.gov/20research/Cropland/SARS1a.htm). This data set is referred to as USDA CDL data in the following text.

The USDA CDL data was derived from high-resolution Landsat TM and ETM+data. The spatial resolution of the data is 30 m (Anonymous, 2006). The main justification for the choice of the CDL data as reference data is that the CDL data identifies as many as 35 crop types and its accuracies for agriculture-related land use classes are high, i.e., between 85% and 95% (Anonymous, 2006). Therefore, it seems advantageous to use the CDL data because the landscape of the four states examined in this study is dominated by crops. Non-agricultural land cover types, on the other hand, are only broadly defined. For instance, woods and woodland pasture are lumped together into the trees class. No information is provided regarding the accuracies for non-agricultural land cover types.

3. Method and data processing

Evidential reasoning (ER) is a powerful approach to data fusion. Several studies have demonstrated that the ER method is applicable to multisource image classification (Le Hégarat-Mascle et al., 2003; Peddle, 1995a,b; Soh et al., 2004). In the remote sensing context, evidential reasoning offers several advantages over traditional classification procedures such as maximum likelihood classifier. First, evidential reasoning is a non-parametric classifier and therefore can handle data which may violate the Gaussian assumption of parametric classifiers (Lee et al., 1987; Srinivasan & Richards, 1990). Second, it can handle data from any number of sources at any scale of measurement. The ER method does not require that input data be independent, as is the case with maximum likelihood classifier (Peddle, 1995b). Third, it has an explicit mechanism for handling information uncertainty through the use of the concept of ignorance. Ignorance describes the incompleteness of one's knowledge as a measure of the degree to which we cannot distinguish between any of the classes (Lein, 2003). Fourth, it can provide several interpretive measures such as support, ignorance and plausibility that can be used to assess classification results (Lein, 2003; Peddle, 1995b).

3.1. Dempster–Shafer theory of evidence

Evidential reasoning is built on the Dempster–Shafer theory of evidence (Dempster, 1967; Shafer, 1976). In Dempster–Shafer theory, a set of mutually exclusive and exhaustive elements, which are referred to as classes in this study, constitutes the frame of discernment, denoted by Θ (Peddle, 1993, 1995a). For example, a set of three classes that we seek to discern would take the form:

$$\Theta = \{\text{crop},\ \text{tree},\ \text{grass}\} \tag{1}$$

The size of the set is the number of singleton classes in the frame of discernment, which is three in this case. A set of size C has exactly 2^C subsets. Thus, the number of subsets for a frame of discernment Θ with three classes is $2^3=8$. These subsets define the power set, symbolized by $P(\Theta)$, and for the above example,

$$P(\Theta) = \{\emptyset,\ \{\text{crop}\},\ \{\text{tree}\},\ \{\text{grass}\},\ \{\text{crop, tree}\},\ \{\text{crop, grass}\},\ \{\text{tree, grass}\},\ \{\text{crop, tree, grass}\}\} \tag{2}$$

Where $\emptyset$ is the null set or an empty set. Note that there is a one-to-one correspondence between the elements of $P(\Theta)$ and the subsets of Θ. A singleton set is a set which has only one class.

The degree of belief in the evidence from a source (e.g., LAI data) in support of a PFT class (e.g., grass) is referred to as the mass (m) committed to that class. The amount of mass is often referred to as evidence measure. A mass can be expressed as a mass function that maps each element of the power set into a real number from 0 to 1, with a higher value indicating a higher level of "belief" expressing the degree to which a pixel belongs to a class. A mass function has the following properties:

(1) The sum of all masses for every subset, X, of the power set is 1:

$$\sum_{X \in P(\Theta)} m(X) = 1 \tag{3}$$

Where $P(\Theta)$ is the power set. In this study, we are interested only in singleton sets or individual classes and, hence, we use C instead of 2^C. A set of 11 PFT classes constitutes the frame of discernment.

(2) The mass of the empty set is defined to be zero:

$$m(\emptyset) = 0. \tag{4}$$

3.2. Implementation of the evidential reasoning (ER) method

In this study, the ER method is implemented in three steps.

3.2.1. Step 1: Generating evidence measures for each PFT from each data source

Transforming input data into evidence is a critical step in evidential reasoning (Peddle, 1995a). Due to its generality, the Dempster–Shafer theory of evidence does not specify how to compute evidence measures. In this study, we developed a

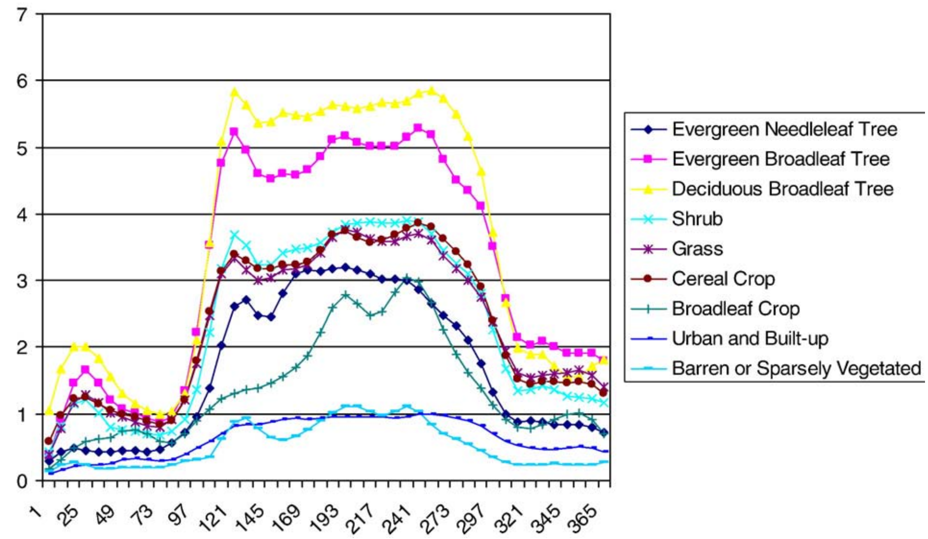

Fig. 1. Plot of the LAI mean vector for each PFT over the year 2001 for Indiana, USA (x-axis = day of the year, y-axis = LAI value).

three-step procedure to derive evidence measures from the input data.

(1) A mean vector over a year is computed for each PFT using each data source. A mean vector contains a set of mean values, with each mean value representing a mean on a particular day of the year. The dimension of a mean vector is defined by the total number of days contained in a data source. The mean value for a PFT on a particular day is computed by first summing all data values of the pixels corresponding to that PFT on that particular day, and then dividing the sum by the number of pixels occupied by that PFT. For example, using the LAI data set, which contains 46 days of data (or 46 layers), and the 1 km MODIS PFT map for Indiana we can construct a mean LAI vector containing 46 mean values for each PFT (Fig. 1). Note that the x-axis of Fig. 1 represents day of the year, and the y-axis the LAI value.

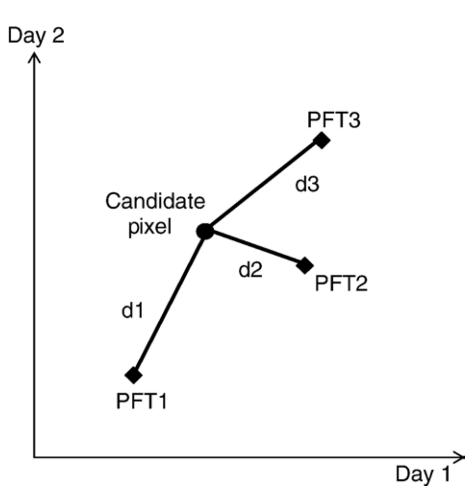

Fig. 2. Illustration of how to calculate the distances of a candidate pixel from the mean vectors of three PFT classes (PFT1, PFT2, PFT3) for two days for a given data source.

(2) The distance of each pixel to the mean vector of each PFT class (i) for each data source is calculated as:

$$d_i = \sqrt{\sum_{k=1}^{m} (\mathrm{PV}_{x,y,k} - \mathrm{MEAN}_{i,k})^2} \tag{5}$$

where $\mathrm{PV}_{x,y,k}$ is the pixel value at location (x, y) on day k; $\mathrm{MEAN}_{i,k}$ is the mean value for PFT class i on day k; m is the number of days used.

For example, suppose we have computed the mean vectors of three PFTs, PFT 1, PFT 2, and PFT 3. We can then calculate the distances of a candidate pixel from the mean vectors of each of the three PFTs, that is, $d1$, $d2$, and $d3$ (Fig. 2).

(3) These distances are finally converted to evidence measures for a set of PFT class labels (X_i) using the following equation:

$$m(X_i) = \frac{1}{d_i \sum_{i=0}^{n} \frac{1}{d_i}} \tag{6}$$

where d_i is the distance from a given pixel to the mean vector of a PFT class i; n is the total number of PFT classes considered.

Fig. 3 shows an example of the evidence measures derived from the MODIS LAI data for Indiana. Note that the higher the grayscale value of a pixel, which appears darker in the image, the higher the belief of that pixel belonging to a particular PFT.

3.2.2. Step 2: Combining evidence from all sources

Once the evidence measures from all data sources for each PFT have been determined in the above step, we need to combine them to generate an overall measure of belief in the evidence. This is achieved by using Dempster's Rule of Combination or orthogonal summation (Dempster, 1967). In this study, the evidence from each data source is combined over

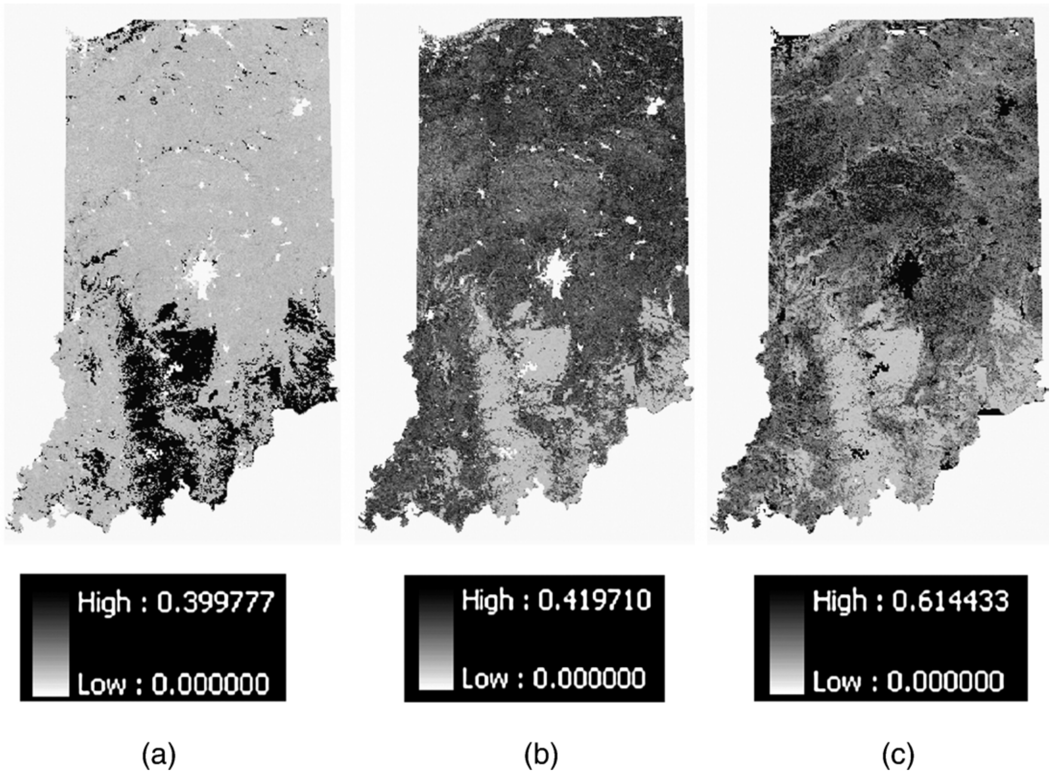

Fig. 3. Evidence measures computed from MODIS LAI data for Indiana, USA showing the mass of each pixel belonging to (a) deciduous broadleaf trees, (b) broadleaf crop, and (c) urban and built-up area.

the same set of singleton class labels (i.e., the 11 PFTs) in the frame of discernment. Suppose $m_1(X)$ is the mass function from source 1 over a set of class labels X, and $m_2(Y)$ is the mass function from source 2 over a set of class labels Y. Then, the equation for computing the orthogonal sum (⊕) of source 1 and source 2 is as follows:

$$m_1 \oplus m_2(Z) = \frac{\sum_{X \cap Y = Z} m_1(X) m_2(Y)}{1 - k} \tag{7}$$

where the sum extends over all class labels whose intersection $X \cap Y = Z$. The set intersections represent common class labels of evidence. $m_1 \oplus m_2(Z)$ is used to determine the combined mass and assigned to a set of class labels Z.

$$k = \sum_{X \cap Y = \phi} m_1(X) m_2(Y) \tag{8}$$

k corrects for any mass that was committed to the empty set (ϕ), and also indicates the extent of conflict between the two sources considered (Shafer, 1976). $k=0$ for complete compatibility and $k=1$ for complete contradiction. Values of $0<k<1$ show partial compatibility.

Orthogonal summation of additional sources is achieved by repeated application of Eqs. (7) and (8). By the commutativity of multiplication, the orthogonal summation from different sources can proceed in any order.

3.2.3. Step 3: Making classification decisions

To classify a pixel into one of the PFT classes, a decision rule is applied to the measure of support and/or plausibility. Support or belief function (Bel) is the total belief of a set and all its subsets. It is defined in terms of the mass:

$$\mathrm{Bel}(X) = \sum_{H \subseteq X} m(H) \tag{9}$$

where H represents any subset of a set X.

The belief function is also referred to as the belief measure, or simply belief. Because we are interested only in singleton sets in this study, the belief in support of a PFT class is equal to the mass committed to that PFT class. For example, Bel ({crop}) = m ({crop}).

Plausibility (Pls) is defined as the degree to which the evidence fails to refute a proposition, X. It is calculated as one minus the support for all other propositions (Shafer, 1976):

$$\mathrm{Pls}(X) = 1 - \mathrm{Bel}(X') \tag{10}$$

where (X') is not (X).

The plausible belief, Pls, stretches belief to the absolute maximum in which the unassigned belief $m(\Theta)$ may possibly contribute to the belief. As such, Bel defines the lower boundary of the support committed to a PFT class labeling proposition, Pls defines an upper boundary, and the range [Bel, Pls] is

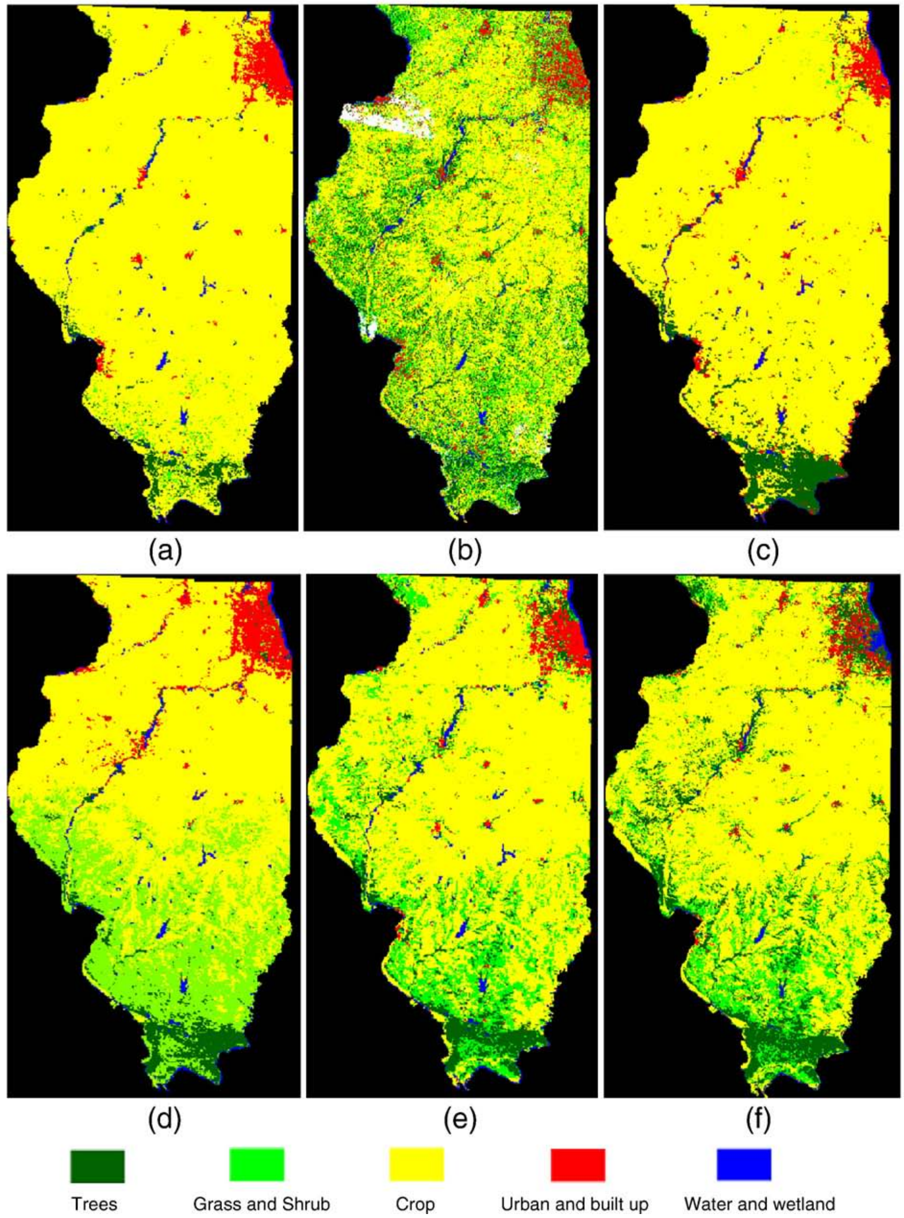

Fig. 4. Comparison of MODIS PFT, USDA CDL data, and ER results for Illinois, USA: (a) MODIS PFT map, (b) USDA CDL data used as "ground truth," and ER results using (c) North America mean vectors, (d) Illinois state mean vectors, (e) Illinois state growing season mean vectors, and (f) Illinois state growing season mean vectors plus weighing factors (weights used: LAI=0.001, EVI=0.6, albedo 1, 2, 3, 4=0.2, albedo 5, 6, 7=0.1).

referred to as evidential interval. In this study, the decision rule is based on maximum support, where the class with the greatest support is assigned as the pixel label.

3.3. Experiment with mean vectors

To determine the mean vectors best suited to the discrimination of PFTs, we computed three sets of mean vectors for each PFT from each data source using the procedure described in step 1 in Section 3.2. First, we computed the mean vectors from each data source for the entire North America. Second, we computed the mean vectors for each of the four states examined in this study. Fig. 1 shows a plot of the LAI mean vectors for Indiana. Third, we calculated the mean vectors for the growing season for each state. State growing season mean vectors were computed by including only data points for the months from April through October.

Fig. 4c, d and e show an example of the ER results using North America mean vectors, state mean vectors, and state growing season mean vectors. For comparative purposes, the MODIS PFT map (Fig. 4a) and the USDA CDL map (Fig. 4b) are also included. As can be seen from Fig. 4, the ER results are sensitive to the mean vectors used. The PFT map generated with North America mean vectors (Fig. 4c) failed to separate grass and shrub and trees from crops. The use of state mean vectors (Fig. 4d) tended to overestimate grass and shrub in the southern half of Illinois, while it identified very little grass and shrub in the northern half of the state. Overall, the use of state growing

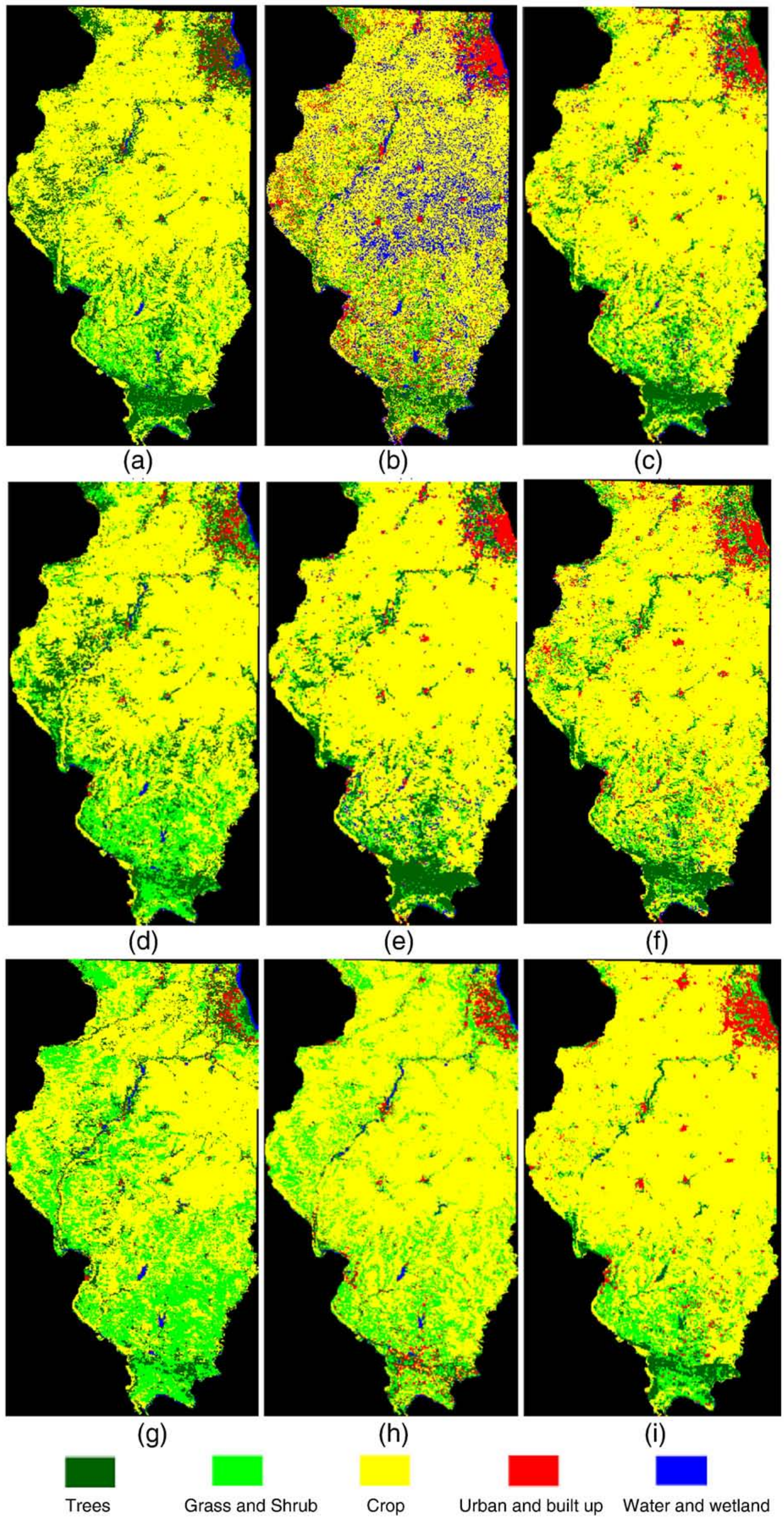

Fig. 5. ER results using Illinois state growing season mean vectors of (a) EVI, (b) LAI, (c) albedo1, (d) albedo2, (e) albedo3, (f) albedo4, (g) albedo5, (h) albedo6, and (i) albedo7.

Table 1
Weights assigned to the nine input data sources

	LAI	EVI	Albedo1	Albedo2	Albedo3	Albedo4	Albedo5	Albedo6	Albedo7
Illinois	0.001	0.6	0.2	0.2	0.2	0.2	0.1	0.1	0.1
Indiana	0.01	0.6	0.1	0.3	0.1	0.1	0.01	0.2	0.1
Iowa	0.1	0.1	0.3	0.15	0.3	0.01	0.01	0.01	0.01
North Dakota	0.98	0.1	0.01	0.01	0.1	0.01	0.01	0.01	0.01

season mean vectors produced the best results (compare Fig. 4e and b).

Similar experiments were carried out for the other three states. A general conclusion from these experiments is that the use of state growing season mean vectors is most effective in discriminating PFTs in the study areas. This result can be attributed to the fact that during the growing season (April–October) the MODIS sensors can better capture the physiological, structural and phenological properties of different PFTs and, therefore, MODIS data captured during this period can do a better job in discriminating PFTs. As such, state growing season mean vectors are used in this study to generate evidence measures in the ER procedure.

3.4. Experiment with weighing factors

To determine the contribution of each data source to PFT classification decisions, we generated nine sets of PFT maps for each state using one data source in each run. For ease of comparison, we again use Illinois as an example. Fig. 5 shows that EVI appears to be very effective in separating major PFTs for Illinois (Fig. 5a). The LAI data, on the other hand, did a poor job in identifying PFTs (Fig. 5b). The seven spectral albedo bands appear generally more effective than LAI, but there are differences between the individual albedo bands (Fig. 5c through i). For example, albedo bands 1 and 2 appear to be more effective than do albedo bands 6 and 7 in discriminating PFTs.

Similar experiments were carried out for the other three states. A general conclusion from these experiments is that the effectiveness of the nine input data sets in discerning PFTs varies greatly from one data source to another. This result suggests that assigning different weights to different sources of input data can enhance classification results. The weights used to generate the final PFT maps are listed in Table 1. These weights were determined based on visual comparisons of the classification results. The closer the PFT map generated with a data set is to the reference data, the greater is the weight assigned to that data source.

3.5. Spatial registration of PFT data and the USDA CDL data

To provide a preliminary assessment of the accuracies of our classification results, we used the USDA CDL data as reference data. Due to the different geoids and different spatial resolutions used in the MODIS products and the USDA CDL data, a spatial registration was carried out. First, the MODIS PFT and our PFT maps were reprojected to the UTM system and WGS 84 spheroid to match those of the USDA CDL data. Second, the USDA CDL data was resampled to a spatial resolution of 25 m, and our PFT maps and the MODIS PFT maps were resampled from 1 km to 25 m. Thus, each original pixel in the PFT maps contains 1600 (40×40) USDA pixels. An overlay of the MODIS PFT maps and the USDA CDL data reveals that the general patterns of land cover features match very well in these two data sets. This is also true of the spatial registration between our PFT maps and the USDA CDL data.

3.6. Recoding of PFT classes and USDA CDL classes

To provide comparability between the MODIS PFT scheme and the USDA CDL scheme, we designed a simplified classification system by recoding certain classes in these two schemes. Table 2 is a translation table showing the relationships between the classes in the simplified system, the MODIS PFT scheme, and the USDA CDL scheme. It is important to note that the merge of PFT classes occurred after running the ER algorithm. In other words, the merge of classes does not affect the availability of the PFT classes generated in the original PFT maps. For example, although the PFT classes of grassland and shrub are merged into a single class (i.e., the grass and shrub class) in the new scheme, the data of both the grassland class and the shrub class generated with the ER method are still available for use.

4. Results

4.1. Area comparison

Table 3 shows the percent areas of the seven aggregated PFT classes in the USDA CDL data, the MODIS PFT, and the PFT classifications generated with evidential reasoning. For simplicity, the PFT classification results generated with evidential reasoning (ER) will be referred to as ER results in the following text.

As can be seen from Table 3, the ER results are much closer to the USDA CDL data in almost all cases. And in several cases, the ER results represent significant improvement over the MODIS PFT. For example, according to the USDA CDL data, three classes including trees, grass and shrub, and crop make up the majority of land (over 90%) of the four states. In the MODIS PFT data, however, crop is identified as the overwhelmingly dominant class, with its area percentage reaching 87% for Indiana, 91% for North Dakota, 92% for Illinois, and over 99% for Iowa. Thus, in terms of the area percentage of the crop class, the absolute discrepancy between MODIS PFT and the USDA CDL data amounts to 33.1%, 37%, 31.4%, and 47.3% for Illinois, Indiana, Iowa, and North Dakota, respectively. The

Table 2
Relationships between the classes in the new scheme used in this study, MODIS PFT scheme, and USDA CDL scheme

New classification scheme	MODIS PFT classification scheme	USDA-NASS CDL classification scheme
Trees (1)	Evergreen Needleleaf Trees (1)	Woods, Woodland pasture (63)
	Evergreen Broadleaf Trees (2)	State 565 Apples (55)
	Deciduous Needleleaf Trees (3)	State 566 Peaches (56)
	Deciduous Broadleaf Trees (4)	State 722 Cottonwood Orchards (71)
Grass and shrub (2)	Grass (6)	Pasture/Range/CRP/Non Ag (permanent & cropland pasture, waste & farmstead) (62)
	Shrub (5)	Pasture/Range/CRP/Non Ag (64)
		Grassland (88)
		Fallow/Idle Cropland (61)
		State 560 CRP (50)
Crop (3)	Cereal crop (7)	Corn (1)
	Broadleaf crop (8)	Cotton (2)
		Rice (3)
		Sorghum (4)
		Soybeans (5)
		Sunflowers (6)
		Peanuts (10)
		Tobacco (11)
		Barley (21)
		Durum Wheat (22)
		Spring Wheat (23)
		Winter Wheat (24)
		Other small grains & hay (25)
		Winter wheat/soybeans double cropped (26)
		Rye (27)
		Oats (28)
		Millet (29)
		Canola (31)
		Flaxseed (32)
		Safflower (33)
		Rapeseed (34)
		Mustard (35)
		Alfalfa (36)
		Beets (41)
		Dry Edible Beans (42)
		Potatoes (43)
		Other Crops (44)
		Watermelon (48)
		State 561 Popcorn (51)
		State 562 Snap Beans (52)
		State 563 Green Peas (53)
		State 564 Pumpkins (54)
		State 567 Sweet Corn-fresh (57)
		State 568 Sweet Corn-processing (58)
		State 569 Other Crops (59)
Urban and built-up (4)	Urban and built-up (9)	Urban (82)
		Roads/railroads (84)
		Buildings/homes/subdivisions (86)
Water and wetland (5)	Water (0)	Water (83)
	Barren or sparse vegetation (11)	Ditches/waterways (85)
		Wetlands (87)
		Mixed water/crops (90)
		Mixed water/clouds (91)
		Aquaculture (92)
Clouds (6)		Clouds (81)
Snow and ice (7)	Snow and ice (10)	

Table 3
Percent area of each PFT class in USDA CDL data (CDL), MODIS PFT (MODIS), and evidential reasoning classifications (ER) for Illinois, Indiana, Iowa, and North Dakota

Class	Illinois			Indiana			Iowa			North Dakota		
	CDL	MODIS	ER	CDL	MODIS	ER	CDL	MODIS	ER	CDL	MODIS	ER
Trees (1)	11.63	2.63	11.61	19.22	9.15	18.04	5.23	0.35	5	0.63	0.17	0.66
Grass and Shrub (2)	19.54	0.87	12.01	23.93	1.36	24.27	26.6	0.09	11.96	45.96	8.94	29.75
Crop (3)	59.04	92.11	72.88	50.2	87.18	64.1	67.76	99.16	82.23	43.42	90.76	62.13
Urban and Built-up (4)	5.64	3.13	2.65	4.51	2.3	3.31	0	0.39	0	1.29	0.08	1.01
Water and Wetland (5)	1.61	1.25	0.86	1.18	0.02	0.28	0.41	0	0.82	7.17	0.04	6.37
Clouds (6)	2.53	0	0	0.97	0	0	0	0	0	1.52	0	0
Snow and Ice (7)	0	0	0	0	0	0	0	0	0	0	0.01	0.07

discrepancy between the ER results and the USDA CDL data is much smaller, i.e., less than 15% for Illinois, Indiana and Iowa, and 18.7% for North Dakota.

The ER method also produced more accurate results for the other two major classes, i.e., the trees class and the grass and shrub class. Take the trees class for example. The discrepancies between the ER results and the USDA CDL data are less than 1.2% for all the four states, whereas the discrepancies between MODIS PFT and the USDA CDL data are 9%, 10%, 5%, and 0.5%, for Illinois, Indiana, Iowa, and North Dakota, respectively. With respect to the grass and shrub class, the differences between the ER results and the USDA CDL data are also smaller than those between MODIS PFT and USDA CDL data, that is, 7.5% (ER) versus 18% (MODIS PFT), 0.3% versus 22%, 14.5% versus 26%, and 16.2% versus 37% for the four states, respectively.

Table 4
Comparison of classification accuracy and Kappa statistic of MODIS PFT and ER results

Class	Producer's accuracy		User's accuracy		Kappa statistics	
	MODIS (%)	ER (%)	MODIS (%)	ER (%)	MODIS	ER
Illinois						
Trees	11.06	25.35	55.17	44.72	0.4759	0.3537
Grass and shrub	1.32	22.77	38.10	35.11	0.2243	0.1870
Crop	98.58	90.45	56.31	65.12	0.1402	0.3136
Urban and built-up	39.44	35.92	66.27	62.96	0.6275	0.5909
Water and wetland	19.50	21.50	63.93	62.32	0.6136	0.5963
Overall accuracy (%)	55.41	57.61				
Overall Kappa					0.2098	0.3153
Indiana						
Trees	39.29	62.83	67.04	58.64	0.5594	0.4471
Grass and shrub	13.25	24.32	30.22	38.36	0.0770	0.1848
Crop	83.23	77.79	56.37	63.99	0.3165	0.4359
Urban and built-up	66.52	37.05	44.61	35.02	0.4014	0.2978
Water and wetland	50.00	8.70	7.67	15.38	0.0623	0.1407
Overall accuracy (%)	48.97	54.95				
Overall Kappa					0.3044	0.3807
Iowa						
Trees	1.55	35.57	37.50	50.92	0.2822	0.4364
Grass and shrub	0.13	30.17	16.67	45.45	−0.1256	0.2633
Crop	99.48	94.13	52.62	69.95	0.0311	0.3856
Urban and built-up					0.0000	0.0000
Water and wetland	0.00	31.00		84.55	0.0000	0.8283
Overall accuracy (%)	51.07	63.65				
Overall Kappa					0.0313	0.3825
North Dakota						
Trees	20.50	36.50	95.35	89.02	0.9502	0.8824
Grass and shrub	15.55	39.53	53.12	52.85	0.2395	0.2352
Crop	94.72	72.52	41.15	46.45	0.0714	0.1552
Urban and built-up	5.63	1.41	100.00	9.68	1.0000	0.0278
Water and wetland	15.43	20.47	68.42	26.44	0.6443	0.1713
Overall accuracy (%)	44.19	46.60				
Overall Kappa					0.1335	0.2012

4.2. Accuracy assessment using random points

Classification accuracies including producer's and user's accuracy and kappa statistic are calculated for the MODIS PFT and our ER results (Table 4). For each state, a total of 3000 reference points were selected from the USDA CDL map using stratified random sampling method. As can be seen from Table 4, the overall accuracies achieved by the ER method are higher than those obtained by MODIS PFT in all the four states. Specifically, the overall accuracies of the MODIS PFT are between 44% and 55% for the four states; these figures have increased to the range of 47% and 64% for the ER results. The biggest improvement occurred in Iowa from 51% to 64%. The overall kappa statistic of the ER results has also increased for all the four states, with the biggest improvement occurring in Iowa from 0.03 to 0.38.

At the class level, crop appears to be extremely well identified in the MODIS PFT product. The producer's accuracies for the crop class in MODIS PFT are over 90% for Illinois, Iowa and North Dakota, and 83% for Indiana. The crop class is also well identified by the ER method. For Illinois and Iowa the producer's accuracies for crop reach 90% and 94%, while these numbers are about 78% and 73% for Indiana and North Dakota, respectively. It is worth noting that significant improvements are achieved by the ER method over MODIS PFT in discerning the trees class and the grass and shrub class, which are the two other major PFT classes in the four states. In terms of producer's accuracy, the maximum improvements occurred in Iowa from 1.6% (MODIS PFT) to 35% (ER) for the trees class and from 0.13% (MODIS PFT) to 30% (ER) for the grass and shrub class.

In comparison to the MODIS PFT, the producer's accuracies for the water and wetland class generated by ER have also increased in Illinois, Iowa and North Dakota but decreased in Indiana. The producer's accuracies for the urban and built-up class identified by ER have slightly decreased in Illinois and North Dakota but significantly decreased in Indiana (30%). A visual comparison of the USDA CDL data and our PFT maps reveals that the ER result actually appears able to detect more spatial details of the urban and built-up areas in Indiana (Fig. 6). This decrease may be attributed to the fact that inadequate urban and built-up reference pixels were selected.

Higher user's accuracies for the crop class are obtained by the ER method in all the four states, with the biggest improvement occurring in Iowa from 53% to 70%. An increase in kappa statistic is also obtained for the crop class by ER in the four states. Large improvements are gained for the grass and shrub class in Indiana and Iowa as well. Kappa statistic for the water and wetland class gained the biggest improvement in Iowa from 0 to 0.83. Considerable improvement also occurred for the trees class in Iowa, whereas slight decreases were observed for Illinois, Indiana, and North Dakota.

4.3. Spatial (per-pixel) comparison

Finally, the MODIS PFT maps and the ER results are compared with the USDA CDL data on a pixel-by-pixel basis (Table 5). Note that the numbers in diagonal cells (bold) are the classification accuracies for each class. As can be seen from Table 5, the classification accuracies for crop in the MODIS PFT maps are extremely high, reaching over 94% for the four states. However, the classification accuracies for the other two major classes, i.e., trees and grass and shrub, are very low in the MODIS PFT maps. For the trees class, the highest accuracy obtained by MODIS PFT is only about 31% for Indiana. The lowest accuracy for the tree class is only 1.4% for Iowa. For the grass and shrub class, the highest accuracy obtained by MODIS PFT is only 13% for North Dakota. The classification

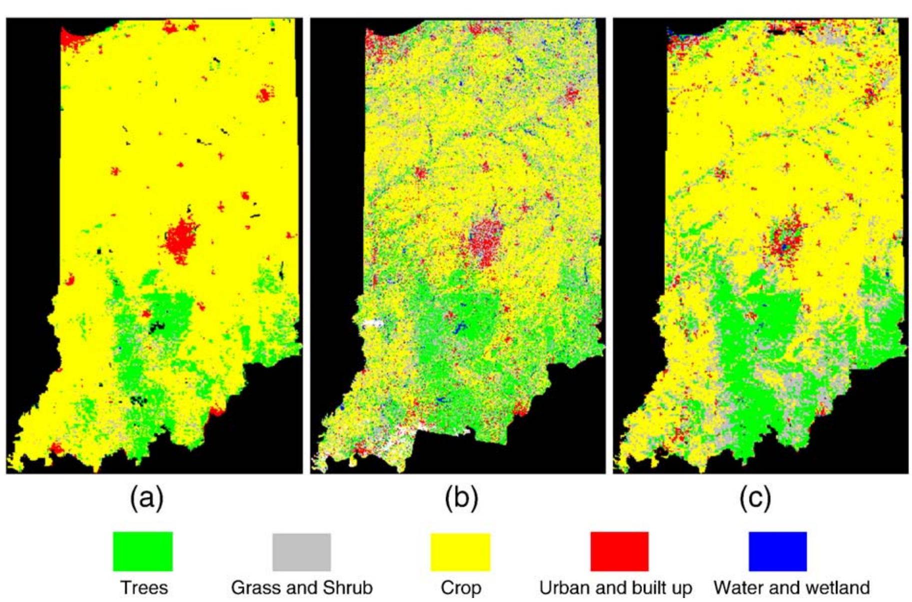

Fig. 6. Comparison of MODIS PFT, USDA CDL data, and ER results for Indiana, USA: (a) MODIS PFT map, (b) USDA CDL data used as "ground truth," and (c) ER results using Indiana state growing season mean vectors plus weighing factors (weights used: LAI = 0.01, EVI = 0.6, albedo 1, 3, 4, 7 = 0.1, albedo 6 = 0.2, albedo 2 = 0.3, albedo5 = 0.01).

Table 5
Spatial (per-pixel) comparison of MODIS PFT and ER results using USDA CDL data as reference data for Illinois, Indiana, Iowa, and North Dakota (row total = 100)

	MODIS PFT						Evidential reasoning					
USDA CDL	Trees	Grass and shrub	Crop	Urban and built up	Water and wetland	Snow and ice	Trees	Grass and shrub	Crop	Urban and built up	Water and wetland	Snow and ice
Illinois (%)												
Trees	**9.51**	1.54	85.31	1.84	1.80		**30.66**	18.32	48.72	1.64	0.66	
Grass and shrub	3.01	**1.43**	89.52	4.63	1.40		16.11	**17.85**	61.12	3.90	1.02	
Crop	0.81	0.54	**97.54**	0.60	0.51		4.76	8.81	**85.19**	1.08	0.16	
Urban and built-up	1.48	0.77	66.07	**28.92**	2.77		20.14	12.08	45.10	**17.57**	5.11	
Water and wetland	11.66	1.86	66.14	3.73	**16.61**		31.08	15.25	39.51	4.76	**9.40**	
Clouds	5.78	0.49	91.95	0.30	1.48		13.23	8.20	77.26	0.72	0.58	
Indiana (%)												
Trees	**30.52**	2.84	65.72	0.89	0.02		**51.59**	17.77	29.06	1.43	0.15	
Grass and Shrub	7.44	**1.73**	87.33	3.48	0.02		17.04	**19.64**	57.21	5.74	0.38	
Crop	2.05	0.56	**97.07**	0.31	0.01		4.67	9.16	**84.96**	1.15	0.05	
Urban and Built-up	4.40	1.43	70.13	**24.00**	0.04		14.51	21.16	41.23	**21.46**	1.64	
Water and Wetland	16.60	1.56	76.56	5.08	**0.21**		29.94	20.34	36.62	9.43	**3.67**	
Clouds	12.26	3.78	82.15	1.48	0.34		19.62	24.73	51.18	4.13	0.35	
Iowa (%)												
Trees	**1.39**	0.28	97.74	0.57	0.01		**26.08**	27.67	45.74	0.00	0.50	
Grass and Shrub	0.58	**0.16**	98.26	1.00	0.00		9.10	**25.51**	63.55	0.00	1.84	
Crop	0.16	0.04	**99.66**	0.14	0.00		1.64	5.26	**92.81**	0.00	0.29	
Urban and Built-up	0.00	0.00	0.00	**0.00**	0.00		0.00	0.00	0.00	**0.00**	0.00	
Water and Wetland	4.78	2.62	91.38	1.22	**0.00**		22.79	40.46	11.27	0.00	**25.48**	
Clouds	0.00	0.00	0.00	0.00	0.00		0.00	0.00	0.00	0.00	0.00	
North Dakota (%)												
Trees	**10.55**	15.28	71.86	0.03	1.92	0.36	**27.87**	26.86	36.90	0.91	2.44	5.04
Grass and Shrub	0.08	**12.77**	86.00	0.05	1.10	0.00	0.46	**37.07**	55.47	0.66	6.31	0.03
Crop	0.07	4.62	**94.75**	0.02	0.54	0.00	0.33	22.22	**72.15**	1.25	4.01	0.03
Urban and Built-up	0.04	17.00	78.77	**2.93**	1.26	0.00	0.24	34.26	50.77	**1.95**	12.77	0.00
Water and Wetland	0.44	5.75	79.79	0.04	**13.98**	0.00	1.75	25.53	53.52	1.77	**17.29**	0.14
Clouds	0.02	11.75	87.10	0.07	1.06	0.00	0.03	40.70	38.43	0.93	19.90	0.00

accuracies of grass and shrub for the other three states are all below 2%.

As shown in the "crop" column of Table 5, a very high percentage of overlapping occurred between MODIS crop class and all other classes in the USDA CDL data. For Illinois, for example, the overlapping between trees and crop is 85%, and the overlapping between grass and shrub and crop is 89%. These numbers suggest that MODIS PFT misclassified a large portion of the four states as crop. It seems clear that the high accuracy for the crop class obtained by MODIS PFT is achieved at the expense of low accuracies of all other classes.

The classification accuracies for the crop class obtained by the ER method are over 85% for Illinois, Indiana, and Iowa. The highest accuracy occurred in Iowa, reaching 93%, and the lowest accuracy is 72% for North Dakota. Significant improvements are also achieved by ER over MODIS PFT for the trees class and the grass and shrub class. The improvements for the trees class are over 17% and, in most cases, over 20%. The improvements for grass and shrub are over 15% for all the four states. In the case of Iowa and North Dakota, the improvements reach around 24%.

It should be noted that some of the ER results, though representing an improvement on the MODIS PFT, are relatively poor (<35%). These poor results may be attributed to the fact only nine MODIS data sets were used in this study as sources of evidence in the ER procedure. Including more evidence layers, especially ancillary data and knowledge about the environmental and ecological conditions of major PFTs (e.g., climate and terrain) may be necessary to further improve the ER results.

5. Conclusions and future research

Plant functional type is a crucial variable required to calibrate, validate and drive various land surface models that provide the boundary conditions for the simulation of climate, carbon cycle and ecosystem change. Using remote sensing techniques to map PFTs is a relatively recent field of research. This paper presents a multisource evidential reasoning (ER) method to map PFTs from a suite of improved and standard MODIS products. The preliminary results from a pilot study conducted in Illinois, Indiana, Iowa, and North Dakota, USA, suggest that multisource data fusion is a promising approach to mapping of PFTs. For several major PFT classes such as crop, trees, and grass and shrub in the study areas, the PFT maps generated with the ER method provide much more spatial details (i.e., smaller spatial units) compared to the MODIS PFT product.

Despite the encouraging results from the pilot study, more work clearly is needed to evaluate the robustness of the proposed method in other regions and at other geographic scales in the future. The four U.S. states examined in this study represent one type of landscape where crops dominate. It seems desirable to test the performance of the ER method in several other regions characterized by different landscapes. For example, the ER method can be applied to the northeastern United States where broadleaf deciduous trees make up a large part of the landscape. Results from multiple regions with different dominant PFTs will allow for a more thorough assessment of the ER approach. Another direction in which the present research can be expanded is to apply the method over larger geographic areas such as the entire North America. Improved mapping of PFTs over North America will have the potential of contributing to other regional earth sciences research programs such as NASA's North American Carbon Program. The production of an improved PFT product at the MODIS scale should also be of interest to the global change research community. As such, more research is needed to explore the feasibility of using the ER approach to generate improved PFT maps at the global scale in the future.

As a first step in the validation of the PFT maps generated with the ER method, the USDA CDL data was used as reference data. Due to lack of information about the accuracies for non-agricultural land cover types in the USDA CDL data, the accuracy analysis for certain classes such as trees and grass and shrub should be considered preliminary. More reference data clearly are needed to validate the ER method in the future. For regions in the United States, certain existing land cover data sets such as the National Land Cover Dataset (NLCD) and the data from Gap Analysis Program (GAP) may be used for this purpose. Using high-resolution Landsat TM and ETM+imagery is another option for relatively small areas. A systematic inventory of PFT-related data collected at the EOS core validation sites and other regional or global validation networks appears to be another promising approach. From a longer term perspective, developing a comprehensive database containing major PFTs representative of different regions around the globe for validation and training purposes is particularly desirable. Such a database may be developed by utilizing certain existing global databases such as the System for Terrestrial Ecosystem Parameterization (STEP) database. The development of a global PFT database may require a considerable amount of resource input, but such an endeavor may prove invaluable for the research community in the long run.

It should be noted that the PFT maps presented in this paper are generated at the local (i.e., state) level, whereas the MODIS PFT is a global product. A rigorous assessment of the accuracies of these two products may not be entirely feasible at this stage. As such, the comparative analyses of the ER results and the MODIS PFT product conducted in this research should be considered preliminary. More rigorous analysis of the performance of the ER method will be provided when it is expanded to generate a global PFT map.

The PFT classification results reported in this paper are based on several high-level MODIS land products available at the present time. It should be noted that, despite the ongoing efforts at improving the quality of MODIS products, almost all MODIS products continue to have large uncertainties that have not been well characterized (Liang, 2003). As such, there is a need to evaluate the effects of uncertainties in the MODIS high-level products on the mapping of PFTs at various geographic scales in the future. Knowledge and information about the magnitude and spatial and temporal distributions of the errors in PFT maps caused by uncertainties in input data may prove valuable to PFT data users.

This research has also revealed that careful selection of input data is critical to fuller realization of the advantages offered by the ER method. For example, our experiment with the mean vectors shows that state growing season mean vectors are more effective than are North America mean vectors and state mean vectors in discriminating PFTs. Our experiment also suggests that for a given area such as a U.S. state, mean vectors computed at local levels (e.g., state mean vectors) appear to be more effective in discerning PFTs than are those computed at more global levels (e.g., North America mean vectors). This observation suggests that the spectral and morphological characteristics of the same PFT captured by remote sensing data may actually vary from one region to another. This raises the issue of how to incorporate regional variations in the spectral and morphological characteristics of PFTs into a classification procedure designed to map PFTs over larger geographic areas (e.g., continents and global). A possible solution is to develop some sort of spatially weighted functions capable of factoring such regional variations into the calculation of evidence measures for the same PFT class in different regions. To develop such spatially weighted functions would require a priori knowledge about how the spectral and morphological characteristics of a PFT vary in relation to locations. How to establish and quantify such relationships in a systematic manner is an issue that requires further research.

Our experiment with the nine input data sets shows that the contribution of different data sources to PFT classification decisions varies. This seems to suggest that to optimize the utilization of the information content of each data source, there is a need to assign different weights to different input data when combining different lines of evidence in the ER procedure. Due to the exploratory nature of the present research, the weighing factors for the nine data sources used in this study were determined based on visual comparisons of classification results. It is clear that a more robust approach is needed to objectively determine optimum weights for different input data in future research. Another issue worth exploring in the future is, for a given input data source (e.g., EVI), whether and to what extent the use of different weights assigned to each PFT class may also affect classification results.

In this study, we used only nine MODIS data sets as sources of evidence to infer PFTs. It seems desirable to evaluate the feasibilities of including additional MODIS and other remote sensing derived products in the ER approach in the future. Furthermore, it should be emphasized that while some of the characteristics exhibited by PFTs such as phenologies and vegetation structure are observable by remote sensing instruments, others may not. For example, certain site-specific environmental and ecological conditions such as temperature, precipitation and elevations appear to be less observable, but they are among the most important factors determining the geographic distribution of PFTs. As such, it seems clear that the use of remotely sensed data alone is insufficient to accurately extract PFT information. This is especially true when mapping PFTs over large geographic areas. What ancillary data should be used and how they can be integrated into the ER approach is another issue that deserves further research.

Acknowledgments

This research was supported through a subcontract of the NASA funded data assimilation project (No. NNG04GL85G). Special thanks for the constructive comments and suggestions from three anonymous reviewers on an earlier draft of this paper.

References

Anonymous (2006). Cropland data layer, metadata.http://www.nass.usda.20-gov/research/Cropland/SARS1a.htm Available at (last accessed, 20 September, 2006).

Bonan, G. B. (1996). *A land surface model (LSM version 1.0) for ecological, hydrological, and atmospheric studies: Technical description and user's guide. NCAR Technical Note NCAR/TN-417+STR.*Boulder, Colorado: National Center for Atmospheric Research (150 pp.).

Bonan, G. B., Levis, S., Kergoat, L., & Oleson, K. W. (2002). Landscapes as patches of plant functional types: An integrating concept for climate and ecosystem models. *Global Biogeochemical Cycles*, *16*(2). doi:10.1029/2000GB001360

Box, E. O. (1996). Plant functional types and climate at the global scale. *Journal of Vegetation Science*, *7*, 309−320.

Caselton, W. F., & Luo, W. (1992). Decision making with imprecise probabilities-Dempster–Shafer theory; and application. *Water Resources Research*, *28*(12), 3071−3083.

Cohen, Y., & Shoshany, M. (2005). Analysis of convergent evidence in an evidential reasoning knowledge-based classification. *Remote Sensing of Environment*, *96*, 518−528.

Dempster, A. P. (1967). Upper and lower probabilities induced by multivalued mappings. *Annals of Mathematical Statistics*, *38*, 325−329.

Denning, A. S., Collatz, G. J., Zhang, C., Randall, D. A., Berry, J. A., Sellers, P. J., et al. (1996). Simulations of terrestrial carbon metabolism and atmospheric CO_2 in a general circulation model. Part 1: surface carbon fluxes. *Tellus*, *48B*, 521−542.

Dickinson, R. E., Shaikh, M., Bryant, R., & Graumlich, L. (1998). Interactive canopies for a climate model. *Journal of Climate*, *11*, 2823−2836.

Fang, H., Liang, S., Townshend, J.R., & Dickinson, R.E. (in press). Spatially and temporally continuous LAI data sets based on an integrated filtering method: Examples from North America. *Remote Sensing of Environment* (in press).

Foley, J. A., Prentice, C. I., Ramankutty, N., Levis, S., Pollard, D., Sitch, S., et al. (1996). An integrated biosphere model of land surface processes, terrestrial carbon balance, and vegetation dynamics. *Global Biogeochemical Cycles*, *10*, 603−628.

Friedl, M. A., McIver, D. K., Hodges, J. C. F., Zhang, X., Muchoney, D., Strahler, A. H., et al. (2002). Global land cover mapping from MODIS: Algorithms and early results. *Remote Sensing of Environment*, *83*(1–2), 287−302.

Gamon, J. A., Huemmrich, K. F., Peddle, D. R., Chen, J., Fuentes, D., Hall, F. G., et al. (2004). Remote sensing in BOREAS: Lessens learned. *Remote Sensing of Environment*, *89*, 139−162.

Giarratano, J. C., & Riley, G. D. (1998). Expert systems: Principles and programming. Boston, MA: PWS-KENT Publishing.

Goldberg, M., Goodenough, D. G., Alvo, M., & Karam, G. (1985). A hierarchical expert system for updating forestry maps with Landsat data. *Proceedings of IEEE*, *73*(6), 1045−1063.

Kucharik, C. J., Foley, J. A., Delire, C., Fisher, V. A., Coe, M. T., Lenters, J. D., et al. (2000). Testing the performance of a dynamic global ecosystem model: Water balance, carbon balance, and vegetation structure. *Global Biogeochemical Cycles*, *14*, 795−825.

Le Hégarat-Mascle, S., Richard, D., & Ottlé, C. (2003). Multi-scale data fusion using Dempster–Shafer evidence theory. *Integrated Computer-Aided Engineering*, *10*, 9−22.

Lee, T., Richards, J. A., & Swain, P. H. (1987). Probabilistic and evidential approaches for multi-source data analysis. *IEEE Transactions on Geoscience and Remote Sensing*, *25*(3), 283−292.

Lein, J. K. (2003). Applying evidential reasoning methods to agriculture land cover classification. *International Journal of Remote Sensing*, *24*, 4161−4180.

Liang, S. (2003). A direct algorithm for estimating land surface broadband albedos from MODIS Imagery. *IEEE Transactions on Geoscience and Remote Sensing*, *41*, 136−145.

Moon, W. M. (1990). Integration of geophysical and geological data using evidential belief function. *IEEE Transactions on Geoscience and Remote Sensing*, *28*(4), 711−720.

Moon, W. M. (1993). On mathematical representation and integration of multiple spatial geoscience data sets. *Canadian Journal of Remote Sensing*, *19*(1), 63−67.

Oleson, K. W., & Bonan, G. B. (2000). The effects of remotely sensed plant functional type and leaf area index on simulations of boreal forest surface fluxes by the NCAR land surface model. *Journal of Hydrometeorology*, *1*, 431−446.

Peddle, D. R. (1993). An empirical comparison of evidential reasoning, linear discriminant analysis and maximum likelihood algorithms for alpine land cover classification. *Canadian Journal of Remote Sensing*, *19*(1), 31−44.

Peddle, D. R. (1995a). MERCURY ⊕: An evidential reasoning image classifier. *Computers and Geosciences*, *21*(10), 1163−1176.

Peddle, D. R. (1995b). Knowledge formulation for supervised evidential classification. *Photogrammetric Engineering & Remote Sensing*, *61*, 409−417.

Peddle, D. R., & Franklin, S. E. (1993). Classification of permafrost active layer depth from remotely sensed and topographic evidence. *Remote Sensing of Environment*, *44*(1), 67−80.

Prentice, I. C, Cramer, W., Harrison, S. P., Leemans, R., Monserud, R. A., & Solomon, A. M. (1992). A global biome model based on plant physiology and dominance, soil properties, and climate. *Journal of Biogeography*, *19*, 117−134.

Running, S. W., & Coughlan, J. C. (1988). A general model of forest ecosystem processes for regional applications. I. Hydrological balance, canopy gas exchange and primary production processes. *Ecological Modeling*, *42*, 125−154.

Running, S. W., Loveland, T. R., Pierce, L. L., Nemani, R. R., & Hunt, E. R., Jr. (1995). A remote sensing based vegetation classification logic for global land cover analysis. *Remote Sensing of Environment*, *51*, 39−48.

Sellers, P. J., Dickinson, R. E., Randall, D. A., Betts, A. K., Hall, F. G., Berry, J. A., et al. (1997). Modeling the exchanges of energy, water, and carbon between continents and the atmosphere. *Science*, *275*, 502−509.

Semenova, G. V., & van der Maarel, E. (2000). Plant functional types — A strategic perspective. *Journal of Vegetation Science*, *11*, 917−922.

Shafer, G. (1976). *A mathematical theory of evidence.* Princeton, NJ: Princeton University Press.

Sitch, S., Smith, B., Prentice, I. C., Arneth, A., Bondeau, A., Cramer, W., et al. (2003). Evaluation of ecosystem dynamics, plant geography and terrestrial carbon cycling in the LPJ dynamic global vegetation model. *Global Change Biology*, *9*(2), 161−185. doi:10.1046/j.1365-2486.2003.00569.x

Smith, B., Prentice, I. C., & Skyes, M. T. (2001). Representation of vegetation dynamics in the modeling of terrestrial ecosystems: comparing two contrasting approaches within European Climate space. *Global Ecology and Biogeography*, *10*, 621−637.

Smith, T. M, Shugart, H. H., & Woodward, F. I. (Eds.). (1997). *Plant functional types: Their relevance to ecosystem properties and global change* New York: Cambridge University Press (369 pp.).

Soh, L., Tsatsoulis, C., Gineris, D., & Bertoia, C. (2004). ARKTOS: An intelligent system for SAR sea ice image classification. *IEEE Transactions on Geoscience and Remote Sensing*, *42*(1), 229−247.

Srinivasan, A., & Richards, J. A. (1990). Knowledge-based techniques for multi-source classification. *International Journal of Remote Sensing*, *11*(3), 505−525.

Strahler, A., Muchoney, D., Borak, J., Friedl, M., Gopal, S., Lambin, E., et al. (1999). *MODIS land cover product algorithm theoretical basis document.* Boston University (Version 5.0).

Sun, W., & Liang, S. (2007). Methodologies for mapping plant functional types. In S. Liang (Ed.), *Advances in Land Remote Sensing: System, Modeling, Inversion and Application,*Springer (in press).

Tian, Y., Dickinson, R. E., Zhou, L., Myneni, R. B., Friedl, M., Schaaf, C. B., et al. (2004). Land boundary conditions from MODIS data and consequences for the albedo of a climate model. *Geophysical Research Letters*, *31*(L05504). doi:10.1029/2003GL019104